Field-induced magnetic phases in the normal and superconducting states of $ErNi_2B_2C$

A. Jensen, K. Nørgaard Toft, A. B. Abrahamsen, D. F. McMorrow, M. R. Eskildsen,* and N. H. Andersen
Materials Research Department, Risø National Laboratory, DK-4000 Roskilde, Denmark

J. Jensen and P. Hedegård
Ørsted Laboratory, Niels Bohr Institute fAPG, Universitetsparken 5, DK-2100 Copenhagen, Denmark

J. Klenke, S. Danilkin, K. Prokes, V. Sikolenko, and P. Smeibidl
Hahn-Meitner Institute, SF-2, D-14109 Berlin, Germany

S. L. Bud'ko and P. C. Canfield
Ames Laboratory and Department of Physics and Astronomy, Iowa State University, Ames, Iowa 50011, USA
(Received 26 September 2003; published 26 March 2004)

We present a comprehensive neutron-diffraction study of the magnetic structures of $ErNi_2B_2C$ in the presence of a magnetic field applied along [010], [110], or [001]. In zero field, the antiferromagnetic structure is transversely polarized with $\mathbf{Q}\approx 0.55\mathbf{a}^*$ and the moments along the *b* direction. At the lowest temperatures, the modulation is close to a square wave, and transitions of *Q* between different commensurable values are observed when varying the field. The commensurable structures are analyzed in terms of a detailed mean-field model. Experimentally, the minority domain shows no hysteresis and stays stable up to a field close to the upper critical field of superconductivity, when the field is applied along [010]. Except for this possible effect, the influences of the superconducting electrons on the magnetic structures are not directly visible. Another peculiarity is that **Q** rotates by a small, but clearly detectable, angle of about 0.5° away from the [100] and the field direction, when the field is applied along [110] and is approximately equal to or larger than the upper critical field.

DOI: 10.1103/PhysRevB.69.104527 PACS number(s): 74.70.Dd, 75.25.+z, 75.30.Kz

I. INTRODUCTION

The rare-earth nickel borocarbides RNi_2B_2C constitute a series of compounds, which exhibit coexistence of magnetic and superconducting phases for $R=$ Dy, Ho, Er, and Tm.[1–3] The substitution with different rare earths scales the magnetic and superconducting properties and gives rise to various fascinating interactions between the two phenomena. The magnetic order of the localized $4f$ moments of the rare-earth ions is mediated by the conduction electrons through the Ruderman-Kittel-Kasuya-Yoshida (RKKY) interaction, which has a maximum around $0.6\mathbf{a}^*$ caused by Fermi surface nesting.[4,5] This implies that an important factor in the interrelation of superconductivity and magnetism in these compounds is the density of states of the conduction electrons at the Fermi surface, which is affected by the gaps induced by a magnetic or a superconducting ordering. In $ErNi_2B_2C$ there is a sharp cusp at T_N in the temperature dependence of the upper critical field H_{c2}, when the field is applied along [001], a minor cusp, when the field is along [100], and only a smooth change of slope, when the field is along [110].[6] The speculation was raised that only an antiferromagnetic state, which is driven by the Fermi surface nesting, is able to cause a sharp cusp in H_{c2}, whereas the antiferromagnetic state in the [100] and [110] case might be different, not dependent on the nesting feature. In this study, the magnetic structures of $ErNi_2B_2C$ are examined, in general, in the presence of a magnetic field, and specifically close to H_{c2}, in order to improve the understanding of the interdependence of superconductivity and magnetism. We found that the antiferromagnetic state has the period of the nesting vector for all three field directions. Alternative explanations for the variations in the cusp in H_{c2} are presented in Sec. VI.

In $ErNi_2B_2C$, the rare-earth ions are placed in a body-centered tetragonal lattice with $a=b=3.502$ Å and $c=10.558$ Å. The ordering wave vector is found to be along the a (b) axis and the ordered moments are along the $b(a)$ axis perpendicular to the ordering wave vector $\mathbf{Q}\approx 0.55\mathbf{a}^*$.[7,8] The Néel temperature is $T_N\approx 6$ K and the superconducting transition occurs at $T_c=11$ K. As early as in 1996, it was proposed that the Er ions develop a small ferromagnetic component below $T_C=2.3$ K in addition to the antiferromagnetic one.[9] This was recently confirmed by neutron-diffraction measurements by Choi *et al.*[10] and by Kawano-Furukawa *et al.*[11] on single crystals in zero field. These neutron-diffraction results have been analyzed in terms of detailed mean-field calculations, and the diffraction patterns detected just above and below the Curie temperature T_C have been identified to derive from two different versions of a commensurable structure with a period of 40 layers along the *a* direction (see Fig. 1 below).[12] The mean-field model is utilized further in the present work in order to help with the interpretation of the different magnetic phases observed.

In the following section, the experimental details are given, followed by a short presentation of the mean-field model with the emphasis on the commensurable magnetic structures that are important for understanding the experiments. The results of the neutron-diffraction experiments are presented in Sec. IV. These results are interpreted and dis-

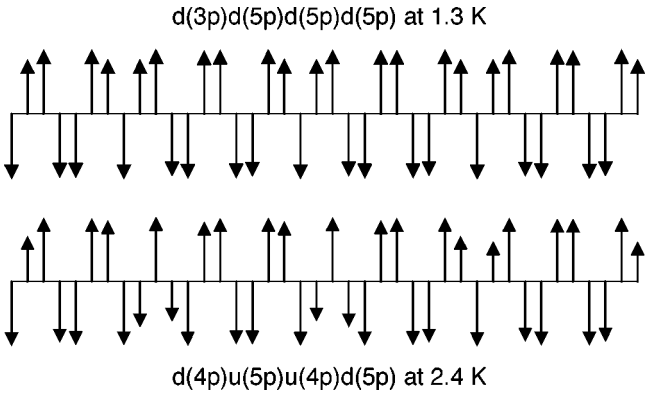

FIG. 1. One period of 40 layers of the $\frac{11}{20}$ zero-field structures calculated below the Curie temperature at 1.3 K, and in the purely antiferromagnetic phase at 2.4 K.

cussed in Sec. V, and comments and concluding remarks are given in the last Sec. VI. In the main part of the paper, the magnitude of the magnetic ordering wave vector Q is given in units of $2\pi/a$.

II. EXPERIMENTAL DETAILS

Here we report on three neutron-scattering experiments carried out on the E1 triple-axis and the E4 two-axis spectrometers, at the Berlin Neutron Scattering Center (BENSC), Hahn-Meitner Institut (HMI). A magnetic field was applied along the crystallographic directions [010], [110], [110] $+22.5°$, and [001] of crystals with dimensions of approximately $2\times3\times0.5$ mm^3. The crystals were grown with 99.5% isotopic enrichment of ^{11}B in order to reduce the neutron absorption.[13] The analysis of the nuclear Bragg peaks shows significant extinction even for the weaker reflections. A wavelength of λ between 2.413 Å and 2.444 Å was selected by the (002) reflection of a pyrolytic graphite (PG) monochromator and higher-order contamination was suppressed by a PG filter in front of the monochromator. The squaring up of the magnetic structure has not been examined since the intensities of the first and higher order reflections are dominated by extinction. The crystals are too perfect for this type of analysis. All measurements in an applied field were performed after zero-field cooling.

The experiments with the field in the ab plane were carried out at the E1 spectrometer using collimators of $70'$, $40'$, $60'$, and $60'$ inserted between source, monochromator, sample, analyzer, and detector, respectively. A horizontal-field cryomagnet with a maximum field of 40 kOe was used. It has large blind angles for neutron diffraction, which restricts the accessible reciprocal space significantly.

For a field along [001], the E4 spectrometer was used with collimators of $40'$ $40'$ $40'$ inserted between the source, the monochromator, the sample, and the detector in order to define the resolution. The vertical field was supplied by a cryomagnet with only a small blind angle and a maximum field of 140 kOe. Results are only reported for fields up to 120 kOe, because the crystal detached at higher fields.

III. MEAN-FIELD MODEL OF THE MAGNETIC STRUCTURES

Many of the special magnetic properties of $ErNi_2B_2C$ are consequences of the strong anisotropy produced by the crystalline field. In the paramagnetic phase, the ground state is a doublet, and an excited doublet is lying only about 0.6–0.7 meV above the ground state. This four-states configuration leads to a four-clock behavior of the moments at low temperatures, i.e., the Er ions are hard to magnetize along the c direction, they are easily magnetized along $\langle100\rangle$, and when the field is applied in the ab plane the magnetization measurements show a $\cos\theta$ dependence.[14] For the field along $\langle110\rangle$ the moments are (approximately) a factor $\sqrt{2}$ smaller than the moments in the $\langle100\rangle$ case. The previous neutron-diffraction experiments have revealed a large third harmonic in the modulation of the ordered moments below ~4 K. Thus, the modulation approaches a square wave at low temperatures, which opens up for the possibility that the magnetic structures lock-in to periods, which are commensurable with the lattice. These commensurable structures may be rather complex and difficult to derive directly from the diffraction experiments. It has previously turned out to be of great value to assist the analysis of diffraction experiments by theoretical model calculations of the stability of the structures which may occur.[15–17] The method consists in calculating the free energies of different commensurable structures within the mean-field approximation, by the application of a straightforward iteration procedure. The results are compared to each other and thereby the most stable structure may be identified.

The mean-field model used here is presented in Ref. 12. The Hamiltonian contains (i) the crystal-field parameters determined from the crystal-field transitions observed by inelastic neutron scattering,[18] and from the high-temperature susceptibilities,[13] (ii) a magneto-elastic quadrupolar term derived from the observed orthorhombic distortion of the lattice in the antiferromagnetic phase,[19] (iii) the classical dipole-dipole interaction as calculated directly, and finally (iv) a Heisenberg two-ion interaction. Most of the ordered structures occurring are described by a wave vector **Q** along the a axis and consist of ferromagnetic sheets perpendicular to **Q**. This means that it is not necessary to distinguish between whether a certain ferromagnetic bc layer belongs to one or the other of the two sublattices of the body-centered-tetragonal lattice, and that only the interplanar couplings between these layers are of importance for the model. The interplanar coupling parameters of the Heisenberg part were derived from the fitting of the zero-field magnetic properties of $ErNi_2B_2C$, as presented in Ref. 12, the magnetization curves,[9,13] and the diffraction results presented here for the magnetic structures appearing in the presence of an applied field.

The calculated results in zero field are based on commensurable structures derived from the basic one at $Q=\frac{1}{2}$. At low temperatures, the moments have an average magnitude of about $7.9\mu_B$, and in one ferromagnetic layer they are either pointing parallel (u) or antiparallel (d) to the b axis (assuming $\mathbf{Q}\|\mathbf{a}$). In the $Q=\frac{1}{2}$ structure, the ferromagnetic

layers perpendicular to **Q** are polarized subsequently $uuddduudd\ldots$ when proceeding along the a direction. Structures with larger values of Q are derived from this structure by a periodic replacement of one or more of the $uu(dd)$ double layers with a single $u(d)$ layer, the so-called spin-slip structures.[20] Important structures are the $Q=\frac{6}{11}$ structure consisting of the 11 layered period $d(uudd)^2uu=d(5p)$ (one moment pointing down followed by five alternating up and down pairs), the 18 layered $Q=\frac{5}{9}$ structure with the period $d(uudd)^2u(dduu)^2=d(4p)u(4p)$, and the 7 layered $Q=\frac{4}{7}$ structure with the period $duuddu=d(3p)$. The zero-field structures at low temperatures have a period of 40 layers and the calculated configurations above and below $T_C\simeq 2.3$ K are shown in Fig. 1. Above T_C, the zero-field structure is described as $d(4p)u(5p)u(4p)d(5p)$, which has no net moment. Below T_C, the structure is $d(3p)d(5p)d(5p)d(5p)$ with a net ferromagnetic moment of $4u$ per 40 atoms (this is estimated to be $0.3\mu_B$ at 2.3 K and $0.6\mu_B$ per Er ion at zero temperature). Numbering the layers from left to right by 1–40, the transition between the two $Q=\frac{11}{20}$ structures is accomplished by a reversal of the moments in the layers 9 and 20.

Based on symmetry considerations, Walker and Detlefs have proposed that weak ferromagnetism in $TbNi_2B_2C$, and possibly also in $ErNi_2B_2C$, is a consequence of a lock-in transition to a commensurable structure with $Q=(m/n)a^*$, where m is even and n is odd.[21] In the case of Er borocarbide, the positions of the higher harmonics in the neutron diffraction measurements[10,11] indicate that the main part of the crystal is ordered in a structure with $Q=0.55$ close to the Curie temperature, both above and below the transition. The presence of minor domains of neighboring commensurable structures implies that the first harmonic shows up as a broadened peak at a wave vector differing slightly from $Q=\frac{11}{20}$. The continuous temperature variation of the position of the first harmonic in Er borocarbide observed in the recent high-resolution x-ray experiment by Detlefs *et al.*[22] is in accordance with this picture. A smooth variation of Q may be produced within a single, slightly disordered, domain by a continuous variation of the number of $(5p)$ relatively to the number of $(4p)$ or $(3p)$ sequences, respectively, above or below T_C. However, the neutron-diffraction results, and also the non-Gaussian line shapes of the peaks in the x-ray experiment, indicate that the system prefers to split up in domains with slightly different compositions of regularly ordered sequences. The neutron-diffraction results of Choi *et al.*[10] indicate that their sample was ordered in the 40-layered structure close to T_C, but slightly mixed with the 51-layered structure with $Q=\frac{28}{51}=0.549$. According to the analysis of Walker and Detlefs a lock-in to the 51-layered structure might be a possible candidate for explaining the ferromagnetic transition, but the mean-field calculations predict that the $d(4p)u(5p)u(4p)d(5p)d(5p)$ version of this structure, which maximizes the distances between the spin-slip layers, only have a net moment and a content of even higher harmonics that are a factor of 5 smaller than observed experimentally below T_C. In the present mean-field model, the $d(4p)u(5p)u(4p)d(5p)d(5p)$ structure is one which may occur above T_C. At the first-order transition at T_C, the positions of the spin-slip layers are rearranged and the 51-layered structure transforms into the $d(3p)d(5p)d(5p)d(5p)d(5p)$ structure, implying an increase of the net moment and the higher even harmonics by the factor of 5. The mean-field analysis of the diffraction experiments indicates that the transition at T_C in $ErNi_2B_2C$ is not explained as a transition from an incommensurable phase to a commensurable one with a ferromagnetic component, as tentatively proposed by Walker and Detlefs. $ErNi_2B_2C$ is in a commensurable phase both above and below T_C, instead the transition is characterized by a rearrangement of the positions of the spin-slip layers of the commensurable structures, $d(4p)\ldots u(4p)\mapsto d(3p)\ldots d(5p)$.[12]

The application of a magnetic field in $ErNi_2B_2C$ will stabilize structures with moments along the field direction, because the strong easy-axis anisotropy makes it more favorable to lengthen and shorten the moments than to rotate them. As the field is increased, the ferromagnetic component will tend to increase. At low temperatures, where the moments are nearly saturated, this may be accomplished by replacing some of the $d(5p)$ sequences with a $d(3p)$ sequence. The magnetic structure is going to consist of a combination of $d(3p)$ and $d(5p)$ sequences with an increasing content of $d(3p)$, until a transition to a pure $d(3p)$ structure is realized. The $d(3p)$ structure has a period of $\frac{4}{7}=0.572$ and a net moment of $1u$ per 7 Er atoms. A further increase of the field introduces combinations of $d(3p)$ and $d(1p)$. A relevant example is the structure $d(1p)d(3p)d(3p)$ with $Q=\frac{10}{17}$. The next structure in this series $d(1p)d(3p)$ has $Q=\frac{3}{5}$, and the even mixture of the two sequences, $d(1p)d(3p)d(3p)d(1p)d(3p)$, leads to $Q=\frac{16}{27}$, close to the maximum Q value encountered in the experiments. Hence, the magnetic structure may gain Zeeman energy on the expense of exchange energy by this increase of Q. Note that sequences with an even number of pairs do not show up in these considerations, because they do not change the resulting value of the ferromagnetic component.

The magnetic system has another possibility for gaining Zeeman energy, namely, by changing a double pair $dduu$ into the sequence $duuu$, i.e., $duudduu\mapsto duuduuu$ in the case of the seven layered structure. This modification does not alter Q, but the magnitude of the first harmonic is reduced.

IV. EXPERIMENTAL RESULTS

In this section, we present neutron-diffraction measurements in the ab plane of $ErNi_2B_2C$ at temperatures between 1.7 K and 7 K, when applying a field of up to 22 kOe along the crystallographic [010] and [110] directions, and up to 120 kOe along the [001] direction. We have also performed a supplementary study with the field applied in a direction lying in between the [010] and [110] directions. The experimental results are summarized by the phase diagrams in Fig. 6 at the end of the section. In zero field, there are two magnetic domains, in which the wave vector of the first harmonic **Q** is either $\mathbf{Q}_A=(Q,0,0)$ or $\mathbf{Q}_B=(0,Q,0)$. The size of the modulation wave vector is constant within error bars at tem-

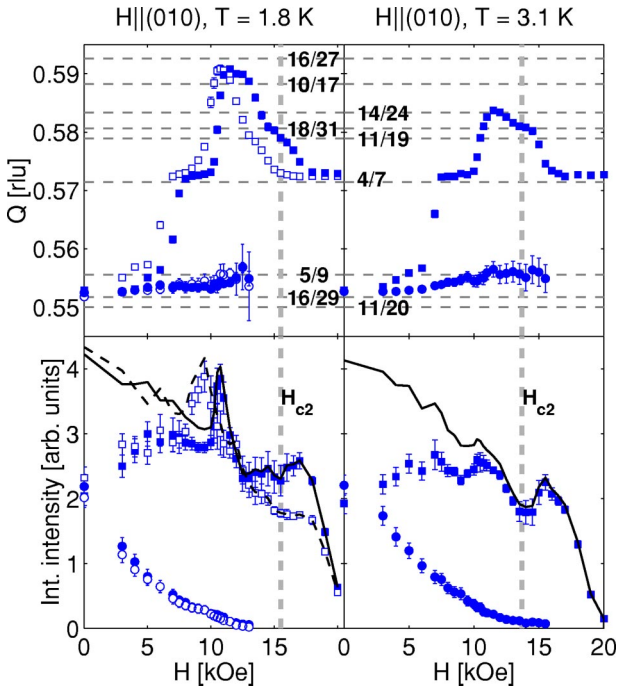

FIG. 2. Positions and integrated intensities of the magnetic reflections of the majority $\mathbf{Q}_A$ domain measured in h scans at $(2-Q,0,0)$ (squares) and of the minority $\mathbf{Q}_B$ domain measured in k scans at $(0,2-Q,0)$ (circles), as functions of a field applied along [010]. The solid symbols represent the data obtained when increasing the field, and the open ones show the decreasing-field data. The measurements were performed only for increasing values of field at 3.1 K. In the lower part of the figure, the sums of the magnetic intensities of the two domains are indicated by lines (solid: increasing field; dashed: decreasing field).

peratures between 1.7 K and 3–4 K. At higher temperatures, Q increases continuously from $Q=0.552$ to $Q=0.555$. The random experimental uncertainty in the determination of Q is of the order 0.0005–0.001, but systematic errors of up to 0.002 have been encountered. The results (not shown here) are in accordance with those previously reported by Choi *et al.*[10] and with the recent x-ray experiments of Detlefs *et al.*[22]

A. Field along [010]

A detailed field analysis of the magnetic reflections at $(200)-\mathbf{Q}_A$ and $(020)-\mathbf{Q}_B$ was performed at several temperatures with the field applied along [010]. In zero field, the magnetic domains with $\mathbf{Q}=\mathbf{Q}_A$ or $\mathbf{Q}_B$ are equally populated, but the application of the magnetic field along [010] suppresses the domain with the magnetic moments perpendicular to the magnetic field, i.e., the $\mathbf{Q}_B$ domain. The intensity of the minority domain is completely suppressed at 13 kOe, as shown in the lower left part of Fig. 2.

Figure 2 presents positions and intensities of the magnetic reflections at $(200)-\mathbf{Q}_A$ and $(020)-\mathbf{Q}_B$ at the temperatures 1.8 K (left) and 3.1 K (right). At 1.8 K, the reflections have been measured both for increasing and decreasing values of the field (solid and open symbols, respectively). The positions are obtained by fitting a Gaussian to the $[h00]$ scans through the magnetic peaks. The scattering intensity due to the minority domain is gradually suppressed by the magnetic field and the value of Q changes slightly from the zero-field value 0.552 to 0.555 during this process. In the case of the majority domain, $\mathbf{Q}_A$ shows several transitions with clear plateaus in between. At 1.8 K, the value of Q changes from 0.552 ($\frac{11}{20}$ or $\frac{16}{29}$) to 0.572 ($\frac{4}{7}$) at 7 kOe, and from this value to 0.590 ($\frac{10}{17}$ or $\frac{16}{27}$) at 11 kOe. At 14 kOe Q is reduced to 0.580 ($\frac{11}{19}$ or $\frac{18}{31}$), and at 17 kOe it reverts to 0.572. The most likely commensurable values, given in the brackets, are indicated in the figure by the dashed lines. The antiferromagnetic ordering disappears at about 21 kOe at that point the sample enters the saturated paramagnetic state. Increasing the temperature to 3.1 K does not change the overall picture, however, the magnetic phase with $Q=0.590$ is not observed, instead $Q=0.584$ appears in a narrow range of fields.

In order to determine which magnetic phase is present at the different values of the field, we need to know the experimental accuracy. All the presented positions are the measured values, corrected for the position of the nuclear Bragg peak. The $\frac{4}{7}=0.5714$ structure, which is the most stable field-induced structure because of its small number of layers in one commensurable period, has an experimental value of Q in the interval 0.5725–0.5730. This indicates a systematic error in the determination of Q of 0.002 in addition to the random one of 0.0005–0.001. This error estimate suggests that the experimental plateau at $Q=0.590$ and 1.8 K is dominantly due to the $\frac{10}{17}=0.5882$ structure rather than to the higher-order $\frac{16}{27}=0.5926$ structure.

Near the transitions from one magnetic period to another, the width of the one-Gaussian fit is found to increase by up to 50%. Due to the restrictions imposed by the blind angles of the magnet, we were not able to move to positions in reciprocal space with a more narrow resolution, but previous preliminary measurements and those presented below when the field is along [110], show that two (or even three) phases are coexisting close to the transitions. Two-Gaussian fits have been performed in these cases. However, it is found that the plots of intensity or position versus magnetic field show the same features as in Fig. 2, and in order to simplify the figure, only the results of the one-Gaussian fits are presented.

The lower part of Fig. 2 presents the integrated intensities of the $(200)-\mathbf{Q}_A$ and $(020)-\mathbf{Q}_B$ magnetic reflections. The intensities are evaluated as the product of the amplitude and the width of the one-Gaussian fits. Numerical integrations or the two-Gaussian fits lead to the same results. The variation of the intensity is probably much effected by extinction: In zero field, the two domains are equally populated, but when one domain is suppressed not all the intensity will appear in the other domain, because the intensity of the larger domain is more affected by extinction. This may explain the decrease of total intensity between 0 kOe and 10 kOe. At 10 kOe and 1.8 K, the total intensity is temporarily regained, which may reflect a reduction of extinction due to the presence of random domains with $Q=0.572$ and $Q=0.590$. At 3.1 K, there is also a peak in the intensity around 10–11 kOe, but much less pronounced. Above 12–13 kOe and below 18 kOe, the total intensity is roughly constant, and in this range the sys-

tem consists of only a single domain with a certain Q, and the minority $\mathbf{Q}_B$ domain has disappeared. Above 18 kOe, the intensity is reduced by the magnetic field until at 20–22 kOe the antiferromagnetic ordering is completely quenched. We have observed an anomalous behavior of the intensity in other cases not included in the figure. One general observation has been that any major change of Q is always accompanied by a peak in the intensity, the one at 1.8 K and 10 kOe being the most extreme example. This general behavior is a further indication that extinction is the main reason for these peaks.

The results at 1.8 K in Fig. 2 are obtained both for increasing and decreasing values of the field. In the case of the majority domain, the hysteresis in the intensity and in the position of the magnetic Bragg peak are concordant with each other. The hysteresis shown by the first-order transitions between different commensurable values of Q is an independent measure for the tendency of the period of the magnetic structure to lock-in to the commensurable values. A detailed neutron-diffraction analysis[23] and the magnetization measurements (see Fig. 7 below) show that the transition to the saturated paramagnetic state at about 20 kOe is of first order, and the smaller intensity observed between 15–20 kOe when reducing the field, are consistent with this first-order nature of the transition. The intensity due to the minority $\mathbf{Q}_B$ domain shows no hysteresis. This is highly surprising. The minority domain was anticipated to be metastable in a field, and after being eliminated completely at high fields, we expected this domain to be energetically unfavorable, until the applied field was reduced to less than ~ 1 kOe. The critical field for the stability of the $\mathbf{Q}_B$ domain has been followed at higher temperatures (measured for increasing values of the field). It is about 13 kOe at 1.8 K and increases to about 14–16 kOe, when the temperature is 3.1 K and 4.1 K, until it finally starts to decrease when the temperature approaches T_N (it is still about 12 kOe at 5.1 K). This critical field is somewhat uncertain to determine, but, clearly, it does not decrease with temperature in the same fashion as the critical field for the $\mathbf{Q}_A$ domain.

B. Field along [110]

In the case where the field is along [110], the two different domains are degenerate, and we observed essentially the same intensities for the magnetic peaks at $\mathbf{Q}_A$ and $\mathbf{Q}_B$. A detailed field and temperature survey was performed for the $(110)-\mathbf{Q}_A$ magnetic reflection. Three different peak positions of the magnetic structure appear as the magnetic field is increased. Figure 3 shows $[h10]$ scans through the $(110)-\mathbf{Q}_A$ reflection at various values of the field at $T=2.0$ K, which represents the three periods of magnetic structure at $h=0.448$, 0.428, and 0.419 rlu corresponding to $Q=0.552$, 0.572, and 0.581. The position and integrated intensity of the first harmonic was determined by fitting one, or, if two phases are present at the same time, two-Gaussian functions to the data points.

With the field properly aligned along [110], we expected to see a smooth variation of the integrated intensity as a function of the applied magnetic field. However, it turned out

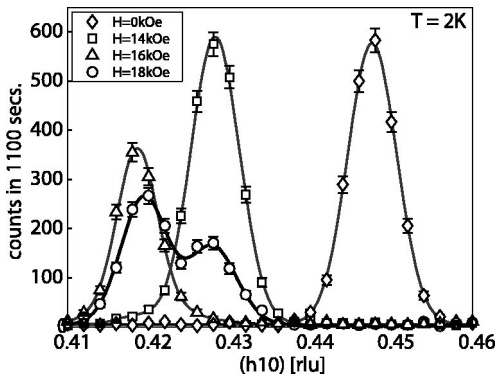

FIG. 3. Field along [110]: $[h10]$ scans of the $(110)-\mathbf{Q}_A$ reflection at $H=0$, 14, 16, and 18 kOe at $T=2$ K. The lines are Gaussian fits to the data.

that there is a loss of intensity around 16 kOe, as may be seen in Fig. 3. The integrated intensity is 40% smaller at 16 kOe than at zero field. In order to clarify this problem, we measured numerous grid scans of the $(110)-\mathbf{Q}_A$ reflection. These show the appearance of a small orthogonal component of the modulation vector at relative high fields. Thus $\mathbf{Q}_A$ changes from $(Q,0,0)$ to $(Q,\delta Q,0)$. An analysis of the magnetic reflection at $(110)+\mathbf{Q}_A$ was performed at several values of field and temperature in order to check for consistency. The finite orthogonal component also appears at the magnetic peaks $(110)-\mathbf{Q}_B$ and $(000)+\mathbf{Q}_B$, giving $\mathbf{Q}_B=(\delta Q,Q,0)$. The upper right part of Fig. 4 shows an example in the case of the $\mathbf{Q}_A$ domain. The grid scan at 2.5 K and 13 kOe determines the center of the peak to be $(1-Q,1,0)$ as expected. As the field is increased to 15 kOe, the position of the reflection shifts to $(0.420,1.005,0)$, which means that the magnetic structure has developed a small orthogonal component $\delta Q\approx -0.005$. Clearly, the presence of the finite orthogonal component explains the observed reduction of the integrated intensity of the $[h10]$ scan at 16 kOe in Fig. 3. We regain 94% of the zero-field intensity at this position. The remaining plots in Fig. 4 show three characteristic variation patterns with field of the principal component Q of the modulation wave vector at $T=1.7$ K, 3 K, and 4.75 K. The Q value is marked by open or solid squares in the respective cases of $\delta Q=0$ or $\delta Q<0$. Open circles represent points where the value of δQ is not known, because no grid scan is performed. At 1.7 K, the $Q=\frac{4}{7}$ structure appears at 11 kOe and is almost completely suppressed at 15 kOe, but reappears at 18 kOe in coexistence with the $Q=0.581$ ($\frac{11}{19}$ or $\frac{18}{31}$) structure up to 20 kOe. The intensity is equally distributed among the two structures in the range of field between 18 to 20 kOe. Note that the $Q=\frac{4}{7}$ magnetic structure, with the short commensurable period of seven layers, has $\delta Q=0$ at all fields and temperatures where it is observed. Whenever δQ is nonzero, in the $\mathbf{Q}_A$ or the $\mathbf{Q}_B$ domain, it is negative. This corresponds to a rotation of $\mathbf{Q}$ away from the direction of the magnetic field, or a rotation of the transverse component of the modulated moments towards the direction of the field. The value $\delta Q\approx -0.005$, corresponding to a ro-

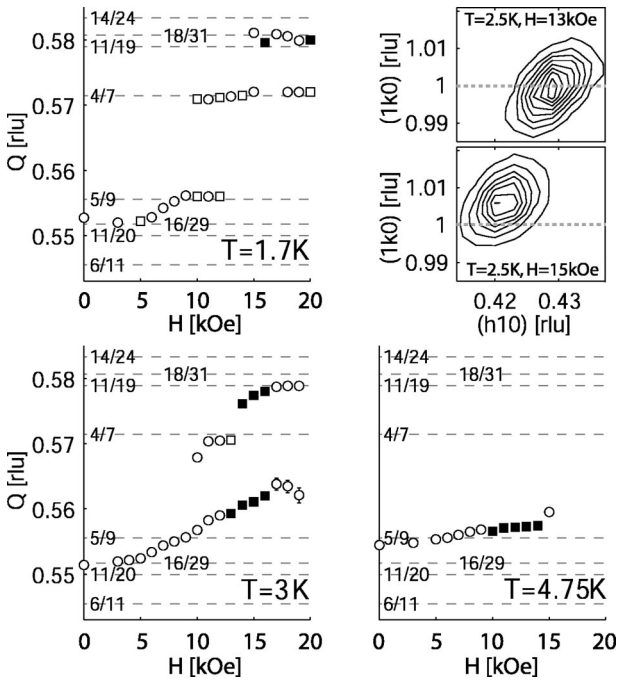

FIG. 4. Field along [110]: The plot in the upper right corner shows two grid scans of the $(110)-\mathbf{Q}_A$ reflection at $T=2.5$ K. At 13 kOe, the peak has its center at $(1-Q,1,0)$, while at 15 kOe the position is $(1-Q,1-\delta Q,0)\approx(0.420,1.005,0)$ corresponding to a finite $\delta Q\approx-0.005$. The other plots show the field dependence of Q at three different temperatures. The markers indicate the value of δQ determined by grid scans at each value of the field: $\delta Q=0$ open square, $\delta Q<0$ solid square. Open circles indicate that no grid scan is performed, so δQ is unknown.

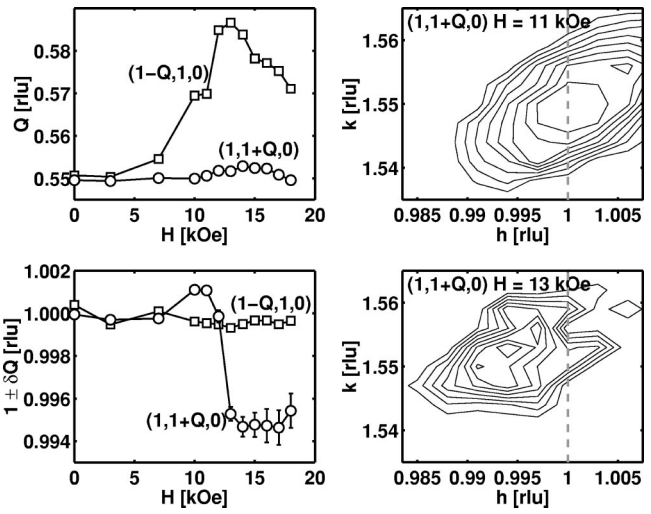

FIG. 5. Field along $[110]+22.5°$ at 1.75 K: The position of the magnetic reflection of the majority (squares) and minority (circles) domains are presented in the left part of the figure. Top: principal periodic modulation Q, and bottom: orthogonal component $1\pm\delta Q$. The right part of the figure presents two grid scans of the minority domain showing that $\delta Q=0$ at 11 kOe and $\delta Q\approx-0.005$ at 13 kOe.

tation of $\mathbf{Q}$ by $-0.5°$, is a typical one, and the largest negative value observed is $\delta Q\approx-0.007$.

C. Field along [110]+22.5°

In order to acquire more information about the unusual rotation of the magnetic ordering wave vector, we have examined the behavior of the magnetic reflections, when applying the field along a direction half way in between the [010] and [110] directions. We performed grid scans of the magnetic reflections at $(110)-\mathbf{Q}_A$ and $(110)+\mathbf{Q}_B$ at base temperature in increasing field, and the results are summarized in Fig. 5. The case $(1-Q,1,0)$ shows the behavior of the $\mathbf{Q}_A$ majority domain, and the grid scans determine the positions of the magnetic reflection to lie between 0.551 to 0.585. No rotation of the magnetic reflection is detected in this domain. In the minority $\mathbf{Q}_B$ domain, indicated by $(1,1+Q,0)$ on the figure, Q changes from 0.550 to 0.553, and, most interestingly, the orthogonal component of the modulation vector is observed to become nonzero, $\delta Q\approx-0.005$, at fields larger than 12 kOe. For both domains, two transition fields are observed at 8 kOe and 12 kOe consistent with the magnetization data.[14]

The magnetic structure in the majority domain behaves roughly in the same way as observed when the field is applied along [010]. In the minority domain the value of Q is nearly constant, as when the field is applied along [010]. The domain is reasonably stable also at high fields, the intensity is still about 20% of the zero-field value at 18 kOe, and, like in the case of field along [110], $\mathbf{Q}$ is rotated at fields above 12 kOe (at 1.75 K). The orthogonal component δQ not only has the same sign, but also the same magnitude as in the [110] case.

D. Field along [001]

The field and temperature dependence of the first harmonic was determined from longitudinal $(h00)$ scans and transverse scans of the $(Q,0,0)$ reflection. The position of the reflection was determined by fitting a Gaussian function to the $(h00)$ scan and the intensity was scaled by the intensity of the transverse scan. As expected from symmetry considerations we did not observe any orthogonal component δQ. When applying the magnetic field along [001] at 1.9 K, the period changes from $Q=0.551$ at zero to $Q=0.555$ at the maximum field of 120 kOe. The temperature dependence of Q at nonzero field is similar to the zero-field variation and the largest value observed is 0.559. At 1.9 K and maximum field, the intensity is only reduced by about 25% from its zero-field value. With the field available, we were only able to reach the Néel temperature at temperatures above 4.5 K. Hence, it requires a very large field along [001] in order to quench the antiferromagnetic ordering. This is qualitatively in accordance with the findings of Schmiedeshoff *et al.*, who determined the field dependence of T_N from kinks in their resistivity measurements.[24] Quantitatively, our experiments indicate the critical field to be larger (above 4.5 K) than determined from the resistivity measurements, and our results are in reasonable agreement with that predicted by the mean-field model, as indicated in the right part of Fig. 6.

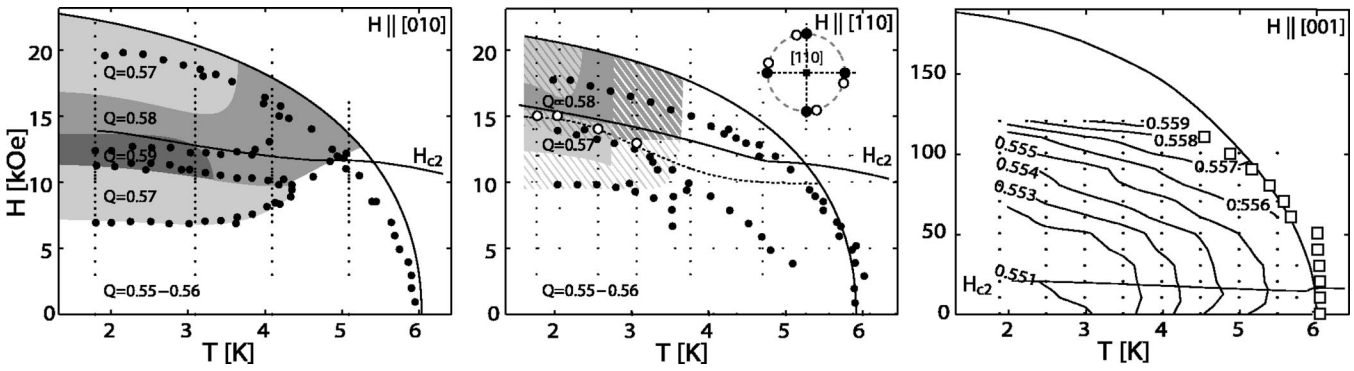

FIG. 6. The magnetic phase diagrams of $ErNi_2B_2C$ for increasing values of applied field along [010] (left), [110] (center), and [001] (right). Small black dots mark the (T,H) points where the measurements were made. The outermost boundary in the [010] and [110] cases marks the experimental points where the intensity of the magnetic phase disappears, and in the last case it is the Néel temperature determined by the mean-field model. The superconducting critical field H_{c2} is marked by a fine line,[6] and the solid circles indicate the magnetic phase lines derived from magnetization measurements.[6] Left, $H\|[010]$: Four commensurable phases are presented in the phase diagram. Center, $H\|[110]$: White and gray areas indicate the existence of one of the three phases, and the striped areas represent coexistence of two of the phases. The modulation wave vector has a finite orthogonal component above the dashed line. Generally, it is not examined below the dashed line, but at fields below the open circles it is determined to be zero. Note that δQ is always zero if $Q=\frac{4}{7}$, which means that in the top left corner the $Q=0.58$ structure with $\delta Q\neq 0$ coexists with the $Q=\frac{4}{7}$ structure, which has $\delta Q=0$. The insert shows schematically how the magnetic reflections are rotated in reciprocal space. Right, $H\|[001]$: Open squares represent the Néel temperature derived from the data, and the lines are contour plots of the values of Q.

The results obtained in the case where the field is applied along [001] are summarized in Fig. 6. This figure also includes an overview of the magnetic phases detected when applying the field along the two other symmetry directions. The phase lines between the different commensurable structures are our best estimates derived from the temperature variation of the magnetic Bragg peak intensities.

V. INTERPRETATION AND DISCUSSION

In this section, we want to discuss the different experimental observations presented in the preceding section. In order to do this we shall utilize the mean-field model and the experimental magnetization curves. The zero-field predictions of the model in comparison with experiments are discussed at lengths in Ref. 12, and we shall here concentrate on the situation in an applied field. Figure 7 shows the magnetization of $ErNi_2B_2C$ measured at 2 K,[9] in comparison with the calculated results derived from the mean-field model.

When the field is applied along [010] (or equivalently along [100]) the domains in which the moments are parallel to the field, or $\mathbf{Q}\|[100]$, are the stable ones. This behavior contrasts with that of a normal antiferromagnet, however, in the present system it is hard to rotate the moments away from the $\langle 100\rangle$ direction, it is much easier to change the magnitude of the moments. The magnetization at 2 K increases steadily until the field is about 7 kOe, where there is a small jump in the curve. The model calculations indicate that this is a transition between the 40-layered structure at $Q=0.55$ to the 7-layered structure at $Q=\frac{4}{7}=0.5714$, which is in accordance with the results of the neutron-diffraction experiments at 1.8 K shown in Fig. 2. These experiments show that Q makes one more jump from $Q=\frac{4}{7}$ to, probably, $\frac{10}{17}$ at 11 kOe. This shows up in the magnetization curve as a small kink as the one at 7 kOe, but the dominating feature is a major jump of $1-2\mu_B$ at 12–13 kOe. The model explains this jump as being due to the $dduu\mapsto duuu$ transition, and the dashed line in Fig. 7 shows the calculated results obtained assuming the seven layered $Q=\frac{4}{7}$ structure to be the stable one. Below the transition, the structure is the $d(3p)=duudduu$ structure, somewhat distorted by the field, which is changed into one with the period $duuduuu$ corresponding to an increase of the average moment by about $1\mu_B$. The solid line shows that the transition is predicted to occur via a number of smaller steps, when the structure (the

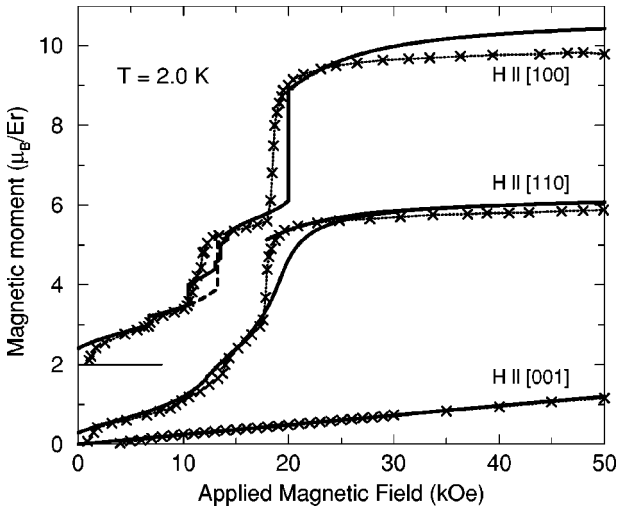

FIG. 7. The magnetization curves of $ErNi_2B_2C$ at 2 K. The crosses connected by dashed lines show the experimental results.[9] The remaining solid and dashed lines are the calculated results. The experimental and theoretical results in the case of $H\|[100]$ have been shifted upwards by 2 units.

one stable in the model) has a longer commensurable period. This transition should in principle also be detectable in the diffraction experiments by a reduction of the scattering intensity by about 20%. Unfortunately, the intensity measurements are much affected by extinction, and it is not possible to decide, whether this predicted reduction in the intensity is occurring or not. Above 13 kOe, the structures with the $duuu$ sequence stay stable until there is a new first order transition, at about $H=20$ kOe, to the paramagnetic phase. In this interval, the model predicts a slight decrease in intensity, in correspondence to the slight increase of the ferromagnetic component.

The variation with temperature of the transitions determined from the magnetization measurements[6] are included in the [010] phase diagram in the left part of Fig. 6. The interpretation of the two lowest magnetic transitions presented above is confirmed by the perfect match between these transitions and the phase boundaries of the $\frac{4}{7}$ structure. The third magnetic transition is the $dduu \mapsto duuu$ transition, which is not detected in the diffraction experiment. The first-order transition to the paramagnetic phase is determined to occur at slightly different values of the field in the two experiments. At low temperatures the difference is about 2 kOe, and here the demagnetization field is estimated to be ~ 1 kOe larger in the present sample than in the one used in the magnetization measurements. This explains directly a part of the difference, but the demagnetization field also smears out the first-order transition and may stabilize intermediate structures. These may cause a small antiferromagnetic scattering peak at fields somewhat above the transition field determined from the magnetization measurements. Neutron-scattering scans performed by Bancroft *et al.* show the intensity contours of all the reflections between (002) and (102) at 1.2 K for fields up to 21 kOe along [100].[25] The behavior of the first-order reflection is in accordance with the present experiments, and an analysis of the higher-order peaks would be a valuable extension of the present investigation.

The diffraction experiments systematically show a minimum or a plateau in the intensities, when the field along [010] is approximately equal to the upper critical field H_{c2} (see Fig. 2). Because of the importance of extinction it is uncertain, but it might be an indication of a slight increase of the antiferromagnetic order component, when the superconducting energy gap at the Fermi surface disappears at the transition to the normal phase.

The most remarkable result obtained in the [010] case is the reversible appearance of the minority $\mathbf{Q}_B$ domain, as discussed in Sec. IV A. The stability of the $\mathbf{Q}_B$ domain up to a field along [010] of about 13 kOe at 1.8 K cannot be explained by the demagnetization field, which is less than 1 kOe at this field and crystal shape. The total magnetoelastic energy involved in the orthorhombic distortion of the crystal, at zero field and 1.8 K, is estimated to be a factor of two larger than the estimated energy difference between the two domains at 10 kOe. Hence, the (meta)stability of the $\mathbf{Q}_B$ domain might be a consequence of the different distortion of the two domains. This effect would decline rapidly with increasing temperatures, in contradiction to that the critical field for the $\mathbf{Q}_B$ domain shows a tendency to increase with increasing temperature. Most importantly, this mechanism leaves no way to explain why the $\mathbf{Q}_B$ domain reappears in a reversible way when the field is reduced. The reversible behavior might suggest that the system is ordered in a double-$\mathbf{Q}$ structure, where the two components may be changed gradually by an external field. However, this possibility is ruled out by the orthorhombic distortion observed in the antiferromagnetic phase at zero field.[19,26] Incidentally, the magnetostriction measurements by Doerr *et al.* show a strong asymmetry of their sample.[26] The volume ratio between the two domains is estimated to be 1:2, as explained by an unequal zero-field population of the two domains of the single-$\mathbf{Q}$ ordered system, and it is noticeable that even the asymmetry is detected to reappear in a reversible way, after the application of a field of 60 kOe. The last possibility for explaining the reversible behavior of the $\mathbf{Q}_B$ domain is to assume that the inhomogeneous Type II phase of the superconductor, in some way, sustains this domain. An indicator of this is that the critical field for the stability of the $\mathbf{Q}_B$ domain, below 5 K, roughly coincides with H_{c2}. The value of $\kappa \approx 8$ is large in this system and the internal magnetic field is not varying much, as soon as the applied field is larger than a few kOe, so the inhomogeneities are mostly connected to the cores of the flux lines. How the cores may be able to stabilize the $\mathbf{Q}_B$ phase is an open question.

When the field is applied along [110], the two domains are both stable, independent of whether the crystal is in the normal or superconducting state. In both domains there is a net ferromagnetic moment making an angle of $\pm 45°$ with the direction of the applied field, at small values of the field. The experimental magnetization curve in Fig. 7 indicates three transitions, when the field is along [110] at 2 K, a weak one at about 10 kOe, one at 14 kOe, and a strong one at about 18 kOe. The model calculations predict only minor steps in the magnetization curve. The calculated free energy of the $\frac{4}{7}$ structure becomes close to the absolute minimum near 10 kOe, and the neutron experiments indicate that this structure is the stable one above this field. This change of the ordering wave vector accounts for the small step in the magnetization curve at 10 kOe. The step at 14 kOe in the magnetization is probably dominantly due to that a major part of the $dduu$ sequences are changed into $duuu$, as the model calculations indicate that this jump is larger than would just derive from the change of Q observed experimentally, from $\frac{4}{7}$ to $\frac{11}{19}$ or $\frac{18}{31}$, see Fig. 4. Hence, the transitions at 10 kOe and 14 kOe are the equivalent ones to those observed at about 7 kOe and 13 kOe, respectively, when the field is applied along [100], as also concluded in Ref. 14. This interpretation is consistent with the coincidence between the low-field magnetization transition with the lower boundary of the $\frac{4}{7}$ phase in the [110] phase diagram of Fig. 6. The second intermediate transition detected in the magnetization measurements, which starts at 14 kOe at 2 K and extends to 4 kOe at 5 K, does not correlate with any of the boundaries between different Q values, in agreement with that this is mainly due to the $dduu \mapsto duuu$ spin-flip modification. A few points in the magnetization data indicate a vertical phase line at about 3.7 K, which we have no explanation for.

The magnetization measurements show that the system

changes from an antiferromagnetic structure to the saturated paramagnetic one at 18 kOe, and the magnetic diffraction peaks disappear around 21 kOe. The model does not predict this transition, but the assumption of a paramagnetic state above 18 kOe leads to a magnetization close to the observed one, as shown by the disrupted solid line in Fig. 7. The model predicts instead a rapid reduction in the magnitude of the oscillations, when the field is increased from 18 to 20 kOe, but the oscillating component remains nonzero even at fields far above 20 kOe. The calculated high-field structure is one where the moments have a ferromagnetic component along the field and a small oscillating one perpendicular to the field. This structure is derived to be stable in spite of that the modulated component along **Q** is a longitudinal one, for which there is a large repulsive energy contribution from the classical dipole interaction, see $\mathcal{J}_{\parallel}(\mathbf{q})$ in Fig. 1 of Ref. 12. In the model, the high-field antiferromagnetic structure becomes unstable if the temperature is increased to 3 K, or if the exchange interaction is reduced by 10%. The [110] phase diagram in Fig. 6 shows that the first-order transition to the paramagnetic phase is determined to lie above the one derived from the magnetization measurements. The discrepancy is larger than in the [010] case, although the demagnetization effects are a factor of $\sqrt{2}$ smaller. This indicates that the tendency for the occurrence of intermediate metastable phases is more pronounced here than in the [010] case, and the high-field antiferromagnetic phase discussed above may be one new possibility.

In the interval between the upper critical field of the superconductor and the critical field for the antiferromagnetic ordering, the neutron experiments show that the ordering wave vector **Q** is no longer along [100] or [010], but is rotated by a small angle of about 0.5° away from the field direction. This rotation happens for all the observed commensurable structures with the exception of the seven layered $Q=\frac{4}{7}$ structure. The rotation may be explained by the gain in Zeeman energy of the commensurable structures, if the moments are rotated by an angle of the same sign and size as **Q** is rotated. This explanation is consistent with all observations: The rotation does not occur, if the field is applied along the *c* axis, or if the angle between the transverse components of the moments and the field is small, as it is in the $\mathbf{Q}_{\mathrm{A}}$ domains, when the field is along [010] or is making an angle of 22.5° with [010] and [110]. In the $\mathbf{Q}_{\mathrm{B}}$ domains, the rotation is observed in the latter case, where the angle is large and the domain is still stable at the required field. The classical dipole-dipole coupling has the potential for producing such a rotation of the moments, but a direct calculation shows that the rotation of the principal axes of the classical coupling matrix at the considered wave vector is negligible (the angle is minus one tenth of the angle by which **Q** is rotated). Hence, the only way to explain the rotation is to assume an additional anisotropic two-ion interaction making up for the inability of the classical coupling to rotate the moments. That such a coupling is a possibility is demonstrated by the stability of the longitudinal polarization of the ordered moments in $TbNi_2B_2C$. The ordering wave vector in the Tb system is practically the same one as in the Er system, but the ordered moments are parallel to **Q**.[8,27] The occurrence of this polarization in $TbNi_2B_2C$ is a direct evidence for the presence of an anisotropic two-ion interaction similar to the classical one, but of opposite sign, so that it more than compensates for the strong reduction of the longitudinal coupling deriving from the classical interaction.

In the case of **Q** making an angle of 0.5° with [100] then the absence of higher harmonics perpendicular to [100] suggests that the 2π phase shift of the magnetic structure per approximately 200 double layers along the [010] direction proceeds in a smooth way. It is not obvious how the commensurable structures may accomplish that, but it is clear that long-period structures, like the 31-layered $Q=\frac{18}{31}$ structure, are less firmly locked to the lattice, and therefore may rotate more easily, than the 7-layered $Q=\frac{4}{7}$ structure. The mean-field model suggests another explanation for why the $Q=\frac{4}{7}$ structure does not rotate. The calculations predict that this structure behaves in a unique way by staying in the *duudduu* configuration all the way up to the transition to the paramagnetic phase, without participating in the $dduu \mapsto duuu$ transition at about 14 kOe. The [110]-results in Fig. 6 show that the rotation of *Q* occurs just above the $dduu \mapsto duuu$ transition at low temperatures. This coincidence indicates that the extra Zeeman-energy gain deriving from the enhancement of the ferromagnetic component perpendicular to **Q**, due to the $dduu \mapsto duuu$ transition, is required in order to make the rotation of *Q* favorable. Therefore, the reason why the $Q=\frac{4}{7}$ structure does not rotate may be a consequence of that the gain in Zeeman-energy is insufficient, as long as the structure stays in the *dduu* phase.

The uniform magnetization created by a field along the *c* axis is small. As seen in Fig. 7, the calculated moment as a function of field along this direction agrees well with the observed magnetization curve. The order parameter of the antiferromagnetic phase decreases gradually as the field is increased until there is a second-order phase transition to the paramagnetic phase. This critical field is calculated to be 183 kOe at 2 K, whereas the experimental value determined by Schmiedeshoff *et al.*[24] from resistivity measurements is 140 kOe. The results of T_{N} from our diffraction experiments, extending up to a field of 110 kOe, are in better agreement with the critical field predicted by the model. The difference between the two experimental sets of data may reflect a dependence of the critical field on the quality of the crystal, but also a minor misalignment of the field may produce a relatively large reduction of the critical field.

The mean-field model accounts rather accurately for the temperature dependence of *Q* at zero and moderated values of the field. In the case of field along [001] the prediction is that the contour curves in the right part of Fig. 6 should have been parallel with the magnetization contours of the antiferromagnetic moment (and T_{N} should have coincided with the contour curve of *Q* equal to 0.555–0.556). The results show that there are some extra changes at large values of the field, which may only be caused by a field-induced modification of $\mathcal{J}_{\perp}(\mathbf{Q})$. When the field is applied in the *ab* plane, the model predicts the right trends in the field dependence of *Q*, that *Q* increases far above the position Q_0 of the maximum in the exchange coupling, because of the gain in Zeeman energy.

The exchange coupling $\mathcal{J}_\perp(\mathbf{q})$ of the model has its maximum at $q=Q_0=0.558$. The model calculations also agree with the tendency of a decrease in Q, when the field is increased above the $dduu \mapsto duuu$ transition around 13–14 kOe. However, the model does not reproduce the stability of the commensurable structures with $Q>\frac{4}{7}$. The larger experimental values of Q observed at ab fields above 10 kOe, indicate that the exchange coupling is changed by the field also in this case. A likely possibility is that the sharp peak in $\mathcal{J}_\perp(\mathbf{q})$ at $\mathbf{q}=\mathbf{Q}_0$ is reduced by the ab field. As discussed in Ref. 12, this peak was introduced in the model, in order to prevent the ordering wave vector to vary too much at zero and low values of the field. A field-induced reduction of the size of the peak in $\mathcal{J}_\perp(\mathbf{q})$ would also improve the comparison of the model and the experiments at fields above 20 kOe along [110].

VI. CONCLUSION

The present experimental and theoretical analysis of the magnetic properties of $ErNi_2B_2C$ has revealed a remarkable variety of different commensurable magnetic structures. The exchange interaction has its maximum at the ordering wave vector of the system close to T_N, that is at about $\mathbf{Q}=0.555\mathbf{a}^*$. The free-energy contributions of the higher harmonics of the ordered moments imply that Q decreases when the temperature is reduced, and it locks-in to the commensurable value $Q=\frac{11}{20}$ below 3–4 K. When a field is applied in the ab plane in this temperature range, the magnetic system may gain Zeeman energy through a reduction of the wavelength of the commensurable structures, and Q is observed to increase by up to 7%–8%.

The mean-field analysis[12] suggests a strong peak in the RKKY interaction near $Q=0.55$, which is likely to be the result of the nesting effects discussed by Rhee *et al.*[4] and by Dugdale *et al.*[5] If this is the case, this would have the consequence that the RKKY interaction should also depend relatively strongly on the energy gaps in the conduction-electron bands created by the spontaneous or field-induced magnetic ordering. The mean-field model, in which the exchange coupling parameters are assumed to be constant, predicts a narrower interval of Q values than that observed at high values of the field. This may be considered to be an indirect evidence for a reduction of the peak in $\mathcal{J}_\perp(\mathbf{Q})$ in the presence of a field, in which reduction is particularly large when the field is applied in the ab plane.

A spontaneous or field-induced ordering of the rare-earth moments in the rare-earth borocarbides has strong consequences for the superconducting electrons. These effects derive from the Anderson-Suhl screening of the electronic susceptibility[28,29] or from the depletion of the number of Cooper-pair states effectuated by magnetic superzone energy gaps, see for instance Refs. 29, 30 or alternatively Ref. 31. Specifically, the behavior of H_{c2} just below T_N is determined by two factors. One is the magnitude of the superzone energy gaps introduced by the antiferromagnetic ordering, which is proportional to the first harmonic of the ordered moments. The other is the rate of depletion in the density of Cooper-pair states produced by these gaps. The first factor is of some importance for explaining the difference in the size of the cusps in H_{c2} at T_N observed experimentally.[6] The first harmonic increases rapidly, when the temperature is reduced below the second-order transition temperature at a constant field applied along [001]. When the field is applied in the ab plane, the transition at T_N is of first order, but the first harmonic below the transition is relatively small. This different behavior may explain a reduction of the cusp by a factor of two, when the field is applied in the ab plane instead of along [001]. At H_{c2}, the induced ferromagnetic moment shifts the conduction spin-up and spin-down bands with respect to each other, due to the RKKY interaction. These spin gaps are much the largest, when the field is in the ab plane. As discussed above, the spin gaps probably have the consequence that the nesting peak in $\mathcal{J}_\perp(\mathbf{Q})$ is reduced. If the nesting feature is diminished, this would also reduce the coupling between the antiferromagnetic and superconducting order parameters, and may therefore result in the further reduction of the cusps in H_{c2} at T_N in the ab case, which is indicated by the experiments.[6]

In contrast, most of the magnetic properties of the present Er system are explained without any reference to the superconducting electrons. There might be some weak influences on the magnitudes of the moments, which are, however, difficult to detect as they probably disappear gradually when approaching the upper critical field.

The spectacular effect of the small-angle rotation of $\mathbf{Q}$ occurs at fields along [110], which are larger than H_{c2}, i.e., in the normal phase. This unexpected observation indicates that the classical dipole interaction cannot be the only anisotropic two-ion interaction of importance in this system. An additional one, such as that responsible for the longitudinal polarization of the ordered moments in $TbNi_2B_2C$, is required in order to account for this particular phenomenon. This rotation of $\mathbf{Q}$ is probably made possible only because of the magnetic $dduu \mapsto duuu$ transition at 14 kOe, by which the Zeeman-energy gain derived from a simultaneous rotation of the moments is increased significantly. The coincidence between the H_{c2} phase line and the field at which the rotation occurs is probably accidental, such as the approximate coincidence between H_{c2} and the $dduu \mapsto duuu$ transition in the case of field along [010]. The abrupt increase of the ferromagnetic component occurring at the $dduu \mapsto duuu$ transition may be able to quench a small superconducting order parameter, implying that the two transitions may occur simultaneously in some parts of the phase diagram.

The second spectacular effect detected in the experiments is the surprising stability and the reversible behavior of the minority $\mathbf{Q}_B$ domain, when the field is applied along [010]. As discussed in the preceding section, it is very unlikely that this phenomenon would have occurred in the normal phase of the magnet. The arguments only leave the explanation that the minority domain, for some unknown reason, is able to survive in parts of the crystal up to a field close to H_{c2}, due to the inhomogeneities introduced by the superconducting Type II phase. This challenging problem needs to be examined in further detail. The hysteresis should be determined at higher temperatures. Also, the hysteresis should be examined while suppressing the superconducting phase, either by dop-

ing, e.g., with cobalt on the nickel site, or by applying an additional magnetic field in the *c* direction.

ACKNOWLEDGMENTS

This work is supported by the Danish Natural Science Council via DanScatt and the Danish Technical Research Council via the Framework Program on Superconductivity. The experiments at BENSC in Berlin were supported by the European Commission under the Access to Research Infra structures Action of the Human Potential Program (Contract No. HPRI-CT-2001-00138). K.N.T. and A.B.A. are supported by the Danish Research Academy, and P.C.C. and S.L.B. are supported by the Director of Energy Research, Office of Basic Energy Science under Contract No. W-7405-Eng.-82.

*Present address: Physics Department, University of Notre Dame, Notre Dame, IN 46556.

[1] R. Nagarajan, C. Mazumdar, Z. Hossain, S.K. Dhar, K.V. Gopalakrishnan, L.C. Gupta, C. Godart, B.D. Padalia, and R. Vijayaraghavan, Phys. Rev. Lett. **72**, 274 (1994).

[2] R.J. Cava, H. Takagi, H.W. Zandbergen, J.J. Krajewski, W.F. Peck, Jr., T. Siegrist, B. Batlogg, R.B. van Dover, R.J. Felder, K. Mizuhasi, J.O. Lee, H. Eisaki, and S. Uchida, Nature (London) **367**, 252 (1994).

[3] P.C. Canfield, P.L. Gammel, and D.J. Bishop, Phys. Today **51** (10), 40 (1998).

[4] J.Y. Rhee, X. Wang, and B.N. Harmon, Phys. Rev. B **51**, 15 585 (1995).

[5] S.B. Dugdale, M.A. Alam, I. Wilkinson, R.J. Hughes, I.R. Fisher, P.C. Canfield, T. Jarlborg, and G. Santi, Phys. Rev. Lett. **83**, 4824 (1999).

[6] S.L. Bud'ko and P.C. Canfield, Phys. Rev. B **61**, R14932 (2000).

[7] J. Zarestky, C. Stassis, A.I. Goldman, P.C. Canfield, P. Dervenagas, B.K. Cho, and D.C. Johnston, Phys. Rev. B **51**, 678 (1995).

[8] J.W. Lynn, S. Skanthakumar, Q. Huang, S.K. Sinha, Z. Hossain, L.C. Gupta, R. Nagarajan, and C. Godart, Phys. Rev. B **55**, 6584 (1997).

[9] P.C. Canfield, S.L. Bud'ko, and B.K. Cho, Physica C **262**, 249 (1996).

[10] S.-M. Choi, J.W. Lynn, D. Lopez, P.L. Gammel, P.C. Canfield, and S.L. Bud'ko, Phys. Rev. Lett. **87**, 107001 (2001).

[11] H. Kawano-Furukawa, H. Takeshita, M. Ochiai, T. Nagata, H. Yoshizawa, N. Furukawa, H. Takeya, and K. Kadowaki, Phys. Rev. B **65**, 180508 (2002); H. Kawano, H. Takeya, H. Yoshizawa, and K. Kadowaki, J. Phys. Chem. Solids **60**, 1053 (1999).

[12] J. Jensen, Phys. Rev. B **65**, 140514 (2002).

[13] B.K. Cho, P.C. Canfield, L.L. Miller, D.C. Johnston, W.P. Beyermann, and A. Yatskar, Phys. Rev. B **52**, 3684 (1995).

[14] P.C. Canfield and S.L. Bud'ko, J. Alloys Compd. **262**, 169 (1997).

[15] J. Jensen and A.R. Mackintosh, *Rare Earth Magnetism: Structures and Excitations* (Oxford University Press, Oxford, 1991).

[16] R.A. Cowley and J. Jensen, J. Phys.: Condens. Matter **4**, 9673 (1992).

[17] J. Jensen, Phys. Rev. B **54**, 4021 (1996).

[18] U. Gasser, P. Allenspach, F. Fauth, W. Henggeler, J. Mesot, A. Furrer, S. Rosenkranz, P. Vorderwisch, and M. Buchgeister, Z. Phys. B: Condens. Matter **101**, 345 (1996).

[19] C. Detlefs, A.H.M.Z. Islam, T. Gu, A.I. Goldman, C. Stassis, P.C. Canfield, J.P. Hill, and T. Vogt, Phys. Rev. B **56**, 7843 (1997); C. Detlefs, D.L. Abernathy, G. Grübel, and P.C. Canfield, Europhys. Lett. **47**, 352 (1999).

[20] D. Gibbs, D.E. Moncton, K.L. D'Amico, J. Bohr, and B.H. Grier, Phys. Rev. Lett. **55**, 234 (1985).

[21] M.B. Walker and C. Detlefs, Phys. Rev. B **67**, 132407 (2003).

[22] C. Detlefs, C. Song, S. Brown, P. Thompson, A. Kreyssig, S.L. Bud'ko, and P.C. Canfield, cond-mat/0306742 (unpublished).

[23] A.J. Campbell, D.McK. Paul, and G.J. McIntyre, Solid State Commun. **115**, 213 (2000).

[24] G.M. Schmiedeshoff, S. Touton, W.P. Beyermann, A.H. Lacerda, S.L. Bud'ko, and P.C. Canfield, Int. J. Mod. Phys. B **16**, 3212 (2002).

[25] N.J. Bancroft, D.McK. Paul, G. McIntyre, C.D. Dewhurst, and R. Cubitt, Pramana, J. Phys. **58**, 907 (2002).

[26] M. Doerr, M. Rotter, M. El Massalami, S. Sinning, H. Takeya, and M. Loewenhaupt, J. Phys.: Condens. Matter **14**, 5609 (2002).

[27] P. Dervenagas, J. Zarestky, C. Stassis, A.I. Goldman, P.C. Canfield, and B.K. Cho, Phys. Rev. B **53**, 8506 (1996).

[28] P.W. Anderson and H. Suhl, Phys. Rev. **116**, 898 (1959).

[29] K. Nørgaard, M.R. Eskildsen, N.H. Andersen, J. Jensen, P. Hedegård, S.N. Klausen, and P.C. Canfield, Phys. Rev. Lett. **84**, 4982 (2000).

[30] K. Machida, K. Nokura, and T. Matsubara, Phys. Rev. B **22**, 2307 (1980).

[31] T.V. Ramakrishnan and C.M. Varma, Phys. Rev. B **24**, 137 (1981).